

## ZnS/ZnO CORE-SHELL STRUCTURES INCORPORATING GRAPHENE ON SAPPHIRE SUBSTRATE

H. CHEN<sup>a\*</sup>, C. C. LU<sup>a</sup>, W.C. WENG<sup>a</sup>, Y. S. TSAI<sup>a</sup>, Y. T. CHEN<sup>a</sup>, W. M. SU<sup>a</sup>,  
C.Y. WENG<sup>a</sup>, C. F. LIN<sup>b</sup>, Y. S. LIN<sup>c</sup>

<sup>a</sup>*Department of Applied Material and Optoelectronic Engineering, National Chi Nan University, Taiwan, ROC*

<sup>b</sup>*Department of Materials Science and Engineering, National Chung Hsing University, Taiwan, ROC*

<sup>c</sup>*Department of Chemical Engineering, Feng Chia University, Taiwan, ROC*

In this study, ZnS/ZnO/graphene/sapphire nanocomposites were formed by sol-gel/hydrothermal methods. To study the influence of various portions graphene layer on ZnS/ZnO/graphene nanostructures, we changed the graphene amounts on the ZnO seed layer solution. To investigate the ZnS/ZnO/graphene/sapphire nanocomposites, multiple analyses including field-emission scanning electron microscopy (FESEM), X-ray diffraction (XRD), photoluminescence (PL), raman spectroscopy (Raman) and contact angle (CA) were performed. Results indicate that denser and more orthogonal ZnS/ZnO/graphene/sapphire structures can be formed with incorporation of graphene.

(Received August 8, 2017; Accepted November 11, 2017)

*Keywords:* Sapphire, graphene, Core-shell structure, ZnS/ZnO, Nanocomposites

### 1. Introduction

Zinc oxide (ZnO) is a multifunctional semiconductor and a large exciton binding energy[1,2] of 60 meV, so ZnO related nanostructures[3] have been widely attracting intensive studies in optoelectronic applications[4-7] because of the wide bandgap[8] of 3.37 eV and it is a hexagonal wurtzite structure[9]. On the other hand, zinc sulphide (ZnS) [10,11] possesses two natural structural phases. One is the zinc blende (sphalerite) structure[12] with a cubic phase[13] and another is wurtzite structure with a hexagonal shape[14]. The bandgap of the cubic and hexagonal phases of ZnS are 3.54 eV and 3.80 eV, respectively. The ZnS/ZnO core-shell[15-17] nanostructures are synthesized by preparation of ZnO nanorods (NRs) and conversion of the ZnO surface into the ZnS shell on the sapphire substrate[18-20]. In this study, we have designed the ZnS/ZnO-based nanocomposites [21] consisting of a graphene layer [22,23] inserted between ZnS/ZnO structures and the sapphire substrate. To investigate the influence of the addition of the graphene layer on ZnS/ZnO core-shell structures, we varied the graphene addition conditions with different amounts of the graphene integrated. To characterize the ZnS/ZnO/graphene/sapphire nanocomposites, multiple material analyses including field-emission scanning electron microscopy (FESEM), X-ray diffraction (XRD), photoluminescence (PL), raman spectroscopy (Raman) and contact angle (CA) were used to examine the nanostructures. Results indicate that more perpendicular ZnS/ZnO core-shell structures can be grown on sapphire substrates with addition of graphene.

---

\*Corresponding author: hchen@ncnu.edu.tw

## 2. Experimental

The sapphire substrates with an area of 2cm×2cm were prepared. To grow ZnO NRs with a graphene layer on the sapphire substrate, the precursor solution contained Zn(CH<sub>3</sub>COO)<sub>2</sub> and two drops of monoethanolamine (MEA) with 60 ml of ethanol was mixed with no graphene, 3 portions (0.3 ml) of graphene, and 6 portions (0.6 ml) of graphene to form the seed layer, respectively. The above-mentioned mixed solutions were spin-coated on the various sapphire substrates. DV-100 (Ted Pella Inc.) pipettes were used to spread graphene on top of the sapphire substrate before the ZnO seed layers were deposited. After the ZnO seed layers with various amounts of graphene were formed, the samples with the ZnO seed layer were placed in solution containing zinc nitrate hexahydrate (Zn(NO<sub>3</sub>)<sub>2</sub>·6H<sub>2</sub>O) and hexamethylenetetramine (HMTA) by hydrothermal methods to grow the ZnO NRs at 80 °C for 1 hour. After that, the ZnO NRs/graphene on the sapphire substrates were immersed in solution of sodium sulfide nonahydrate (Na<sub>2</sub>S·9H<sub>2</sub>O) at 70 °C for 5 min. With Na<sub>2</sub>S dissolving out S<sup>2-</sup> ion source to convert ZnO to ZnS [25], the ZnS/ZnO/graphene/sapphire nanocomposites can be formed based on the following chemical reaction formula:



## 3. Results and discussion

To observe the surface morphologies of the ZnS/ZnO core-shell grown in four different conditions, field-emission scanning electron microscope (FESEM) was used to view the morphologies of the nanostructures.

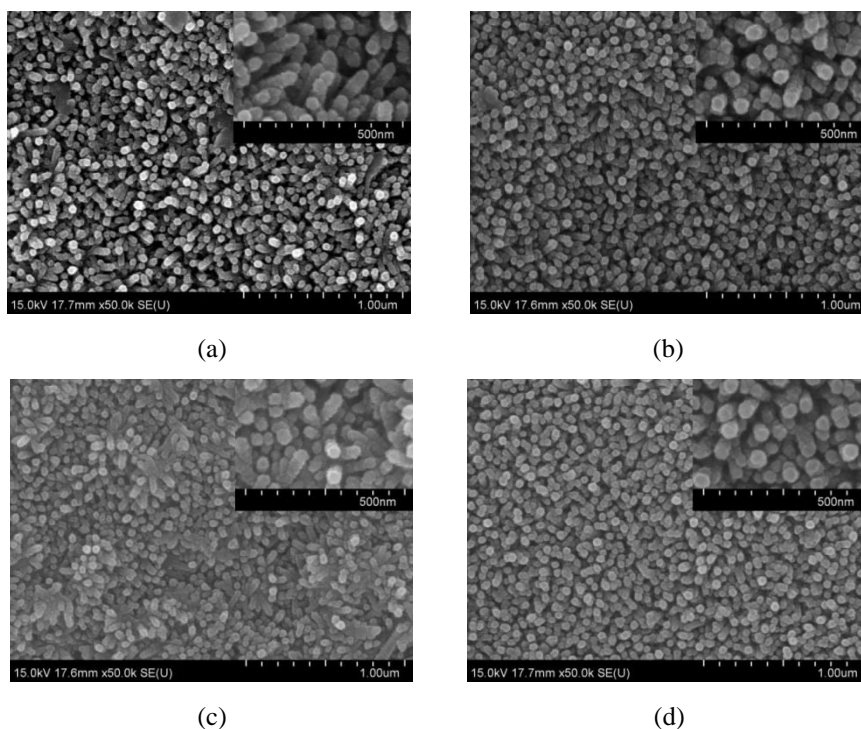


*Fig. 1 FESEM images of the surface of the ZnS/ZnO core-shell on the sapphire substrates with the seed layer (a) with a graphene layer (b) without graphene (c) with 3 portions (0.3 ml) of graphene and (d) with 6 portions (0.6 ml) of graphene in various magnification rates.*

As shown in Fig. 1 (a), arrays of ZnO nanorods with coated ZnS were synthesized on the sapphire with spreading a graphene layer on bottom of ZnS/ZnO structures. By contrast, ZnS/ZnO core-shell without a graphene layer showed better growth for NRs grown on sapphire substrates, as shown in Fig. 1(b). Moreover, ZnO NRs with the seed layer incorporated with 3 and 6 portions of graphene by Fig. 1(c) and (d). Compared with ZnS/ZnO nanostructures with spreading a graphene layer on bottom, ZnS/ZnO nanostructures with ZnO seed layer incorporating 6 portions of graphene possessed the densest and the most orthogonal structure.

To study the crystalline structures of ZnS/ZnO incorporating graphene and without graphene, XRD was used to examine the material quality as shown in Fig. 2. Consistent with FESEM results, ZnS/ZnO structures with 6 portions of graphene added into the ZnO seed layer solution had the strongest (002) c-axis phase and (103). Moreover, ZnS/ZnO structures with 6 portions of graphene added into the ZnO seed layer solution had strongest ZnS (111) phase.

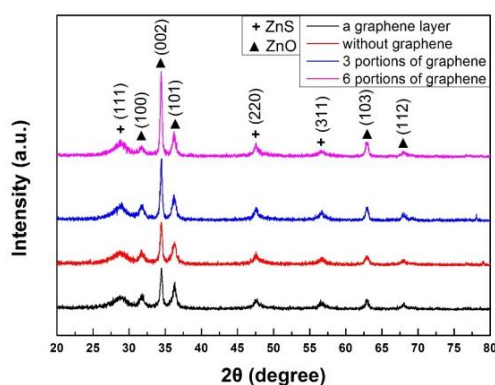


Fig. 2 XRD spectra of the ZnS/ZnO core-shell on the sapphire substrates with four different conditions of graphene. (1 portion = 0.1 ml of graphene)

In addition, the optical properties of the ZnS/ZnO structures with adding various portions of graphene into the seed layer were investigated by PL measurements as shown in Fig. 3. The PL peak of the spectrum around 375 nm showed the near band edge (NBE) emission, and the peak around 570 nm in the spectrum represented the defect luminescence. The peak of NBE/defect emission ratio of the ZnS/ZnO structures with 6 portions of graphene added into the ZnO seed layer solution was stronger than that with 3 portions of graphene added into the ZnO seed layer solution. Therefore, the graphene-incorporated ZnS/ZnO with 6 portions had the better material properties corresponding with FESEM and XRD analyses.

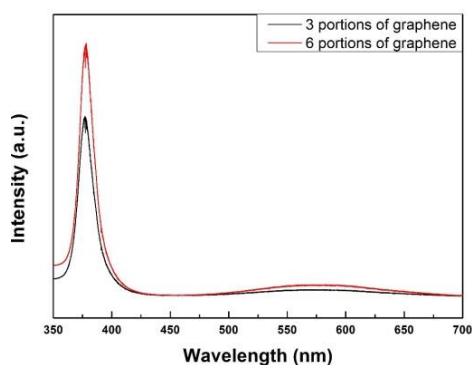


Fig. 3 PL measurements of the ZnS/ZnO core-shell on sapphire substrates with the seed layer incorporating various amounts of graphene. (1 portion = 0.1 ml of graphene)

Moreover, the Raman spectra of the graphene-incorporated ZnS/ZnO as shown in Fig. 4. Peaks of 475, 570, 1145, and 1720  $\text{cm}^{-1}$  in Raman spectrum signifies the ZnO nanostructure while 350 and 695  $\text{cm}^{-1}$  of ZnS structures could be detected. The increase of graphene concentration resulted in a stronger peak of 1720  $\text{cm}^{-1}$ . The peak of 570  $\text{cm}^{-1}$  represents C-axis for ZnO, while the peak of 1145 and 1720  $\text{cm}^{-1}$  indicates multiple photon vibrations and asymmetric multiple photon vibrations, respectively.

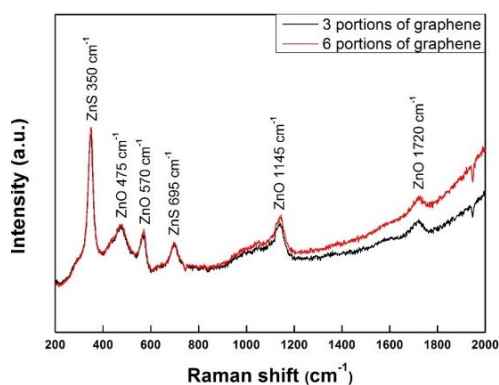


Fig. 4 Raman analysis of the ZnS/ZnO core-shell on sapphire substrates with the seed layer incorporating various amounts of graphene. (1 portion = 0.1 ml of graphene)

Finally, contact angle measurements for the hydrophobicity of various nanostructures are shown in Fig. 5(a), (b), (c), and (d). Incorporating graphene into the ZnO seed layer solution might cause lower hydrophobicity of the ZnS/ZnO core-shell nanostructures so the contact angles became smaller as shown in Fig. 5(c) and (d). On the other hand, spreading a graphene layer on bottom of ZnS/ZnO structure may enhance the hydrophobicity as shown in Fig. 5(a).

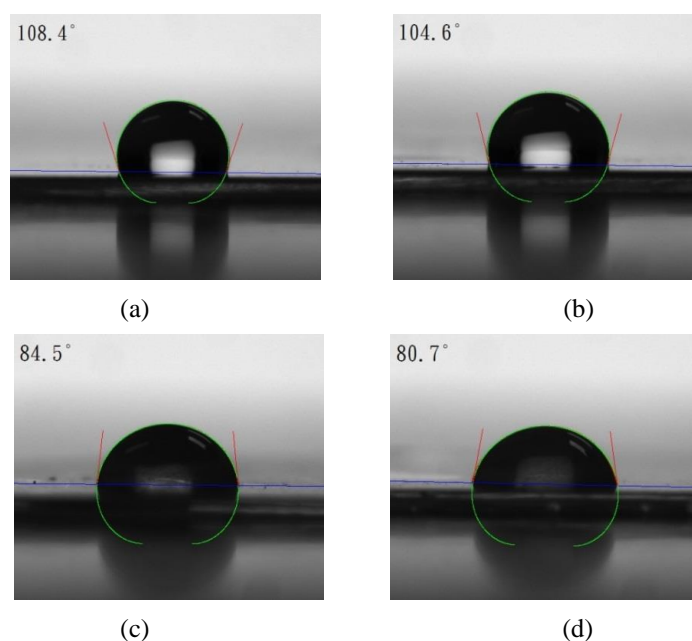


Fig.5 Surface contact angle measurements of the surface of the ZnS/ZnO core-shell on the sapphire substrates with the seed layer (a) with a graphene layer on bottom (b) without graphene (c) with 3 portions (0.3 ml) of graphene and (d) with 6 portions (0.6 ml) of graphene.

#### 4. Conclusions

In this research, ZnO/ZnS core-shell structures were grown on the sapphire substrates incorporating graphene. Results indicate that the morphology of ZnS/ZnO core-shell growth was modulated by addition of different amounts of the graphene into seed layer by hydrothermal method.

In addition, multiple material characterizations show that stronger crystalline structures, higher hydrophilic properties, and higher near band edge emission by incorporating graphene into the seed layer. The ZnS/ZnO core-shell nanostructures with graphene show promises for future optoelectronic and biomedical device applications.

#### Acknowledgements

This work was supported in part by the Ministry of Science and Technology of Taiwan, ROC under Contract No: MOST 104-2221-E-260-002 -MY3.

#### References

- [1] J. Min, B. Wang, X. Liang, Y. Zhao, Z. Zhu and S. Hu, *Rare Metal Materials and Engineering* **40** (5), 761 (2011).
- [2] H. W. Choi, N. D. Theodore, S. Das, A. Dhar and T. Alford, *Journal of Crystal Growth* **406**, 26 (2014).
- [3] L. Vayssieres, *Advanced Materials* **15** (5), 464 (2003).
- [4] C. Gray, J. Cullen, C. Byrne, G. Hughes, I. Buyanova, W. Chen, M. O. Henry, E. McGlynn, *Journal of Crystal Growth* **429**, 6 (2015).
- [5] I. Kazeminezhad and A. Sadollahkhani, *Materials Letters* **120**, 267 (2014).
- [6] H. Ikeri, A. Onyia and P. Asogwa, *Chalcogenide Letters* **14** (2), 49 (2017).
- [7] A. Sadollahkhani, O. Nur, M. Willander, I. Kazeminezhad, V. Khranovskyy, M. O. Eriksson, R. Yakimova, P.-O. Holtz, *Ceramics International* **41** (5), 7174 (2015).
- [8] K. S. Rathore, D. Patidar, Y. Janu, N. Saxena, K. Sharma, T. Sharma, *Chalcogenide Letters* **5** (6), 105 (2008).
- [9] X. Huang, M. Wang, M.-G. Willinger, L. Shao, D. S. Su and X.-M. Meng, *ACS nano* **6**(8), 7333 (2012).
- [10] A. Abbad, H. Bentounes, W. Benstaali, S. Bentata and B. Bouadjemi, *Chalcogenide Letters* **12** (6) (2015).
- [11] L. Kong, J. Deng, L. Chen, *Chalcogenide Letters* **14** (3) (2017).
- [12] P. Guo, J. Jiang, S. Shen and L. Guo, *International Journal of Hydrogen Energy* **38** (29), 13097 (2013).
- [13] J. S. Cruz, D. S. Cruz, M. Arenas-Arrocena, F. De Mooureflores and S. M. Hernandez, *Chalcogenide Letters* **12** (5), 277 (2015).
- [14] P. V. Raleaooa, A. Roodt, G. G. Mhlongo, D. E. Motaung, R. E. Kroon and O. M. Ntwaeaborwa, *Physica B: Condensed Matter* **507**, 13 (2017).
- [15] M. Sookhakian, Y. Amin, W. Basirun, M. Tajabadi and N. Kamarulzaman, *Journal of Luminescence* **145**, 244 (2014).
- [16] M.-K. Tsai, W. Huang, S.-Y. Hu, J.-W. Lee, Y.-C. Lee, M.-H. Lee and J.-L. Shen, *Micro & Nano Letters* **11**(4), 192 (2016).
- [17] T. Yu, K. Wang, Y. Chen, M. Sheu, H. Chen, *Chalcogenide Letters* **14**(4) (2017).
- [18] Z. Bandić, E. Piquette, J. McCaldin and T. McGill, *Applied physics letters* **72** (22), 2862 (1998).
- [19] G. Lee, T. Kawazoe and M. Ohtsu, *Solid state communications* **124** (5), 163 (2002).
- [20] Y.-C. Liang, C.-C. Wang and Y.-J. Lo, *Ceramics International* **42** (14), 15849 (2016).

- [21] V. An, B. Liu, *Chalcogenide Letters* **12** (12), 639 (2015).
- [22] H. Chen, Y. Y. He, M. H. Lin, S. R. Lin, T. W. Chang, C. F. Lin, C.-T. R. Yu, M. L. Sheu, C. B. Chen and Y.-S. Lin, *Ceramics International* **42** (2), 3424 (2016).
- [23] T.-Y. Yu, M. R. Wei, C. Y. Weng, W. M. Su, C. C. Lu, Y. T. Chen and H. Chen, *AIP Advances* **7**(6), 065110 (2017).
- [24] K. Bramhaiah, V. N. Singh and N. S. John, *Physical Chemistry Chemical Physics* **18** (3), 1478 (2016).
- [25] A. Brayek, M. Ghoul, A. Souissi, I. B. Assaker, H. Lecoq, S. Nowak, S. Chaguetmi, S. Ammar, M. Oueslati, R. Chtourou, *Materials Letters* **129**, 142 (2014).